

Section 1

LASER SYSTEM REPORT

1.A OMEGA Facility Report

Tests to evaluate the spatial intensity distribution of an OMEGA beam at the location of a target were conducted this quarter. In addition, the 24 beam laser was prepared for the first series of target experiments scheduled for later in the year.

The near field photographs discussed in Volume 5 of the LLE Review were digitized and processed on the LLE Cyber 175. Extensive cross checks of the calibration of this process were performed. It is anticipated that these photographs will provide the data to normalize several beam propagation codes during the following quarter.

A series of shots were taken on OMEGA to study the optical properties of the laser beam at the end of the laser and at the target chamber focus lens. Near field cameras were used at both locations to measure the pulsed beam intensity distribution and shearing interferometry was used at both locations to measure the pulsed beam phase distribution. In addition, far field array cameras recorded the intensity distribution from best focus to approximately 1,200 μm inside of focus on the OMEGA focus lens. This data is now being reduced to compare to calculations and to provide a baseline characterization of a typical OMEGA beamline at 100 psec and at 600 psec.

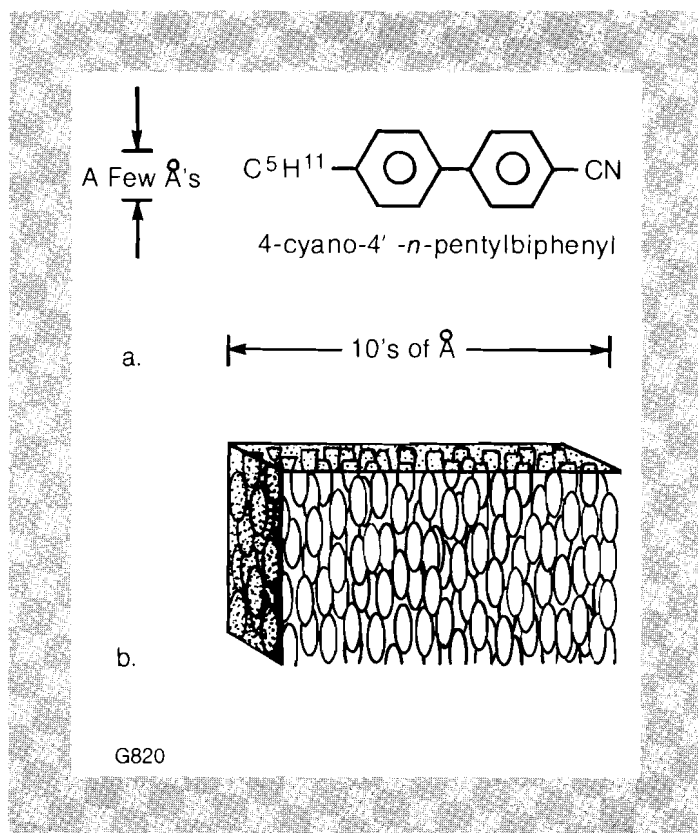
1.B Liquid Crystal Devices for High Powered Lasers – Part 2: Waveplates

The ability to manipulate the state of polarization of laser radiation is fundamental to successful operation of large laser systems like LLE's OMEGA. Propagation of circularly polarized light through large rod amplifiers maximizes system output power.¹ Electro-optic switching of linearly polarized light with Pockels cells² suppresses amplified spontaneous emission (ASE)³ and provides isolation between amplification stages. Rotation of the plane of polarization for linearly polarized light incident on beamsplitting mirrors determines beam energy balance among the arms of multiple beam systems. This control over the polarization state of light in a laser system is achieved through the use of passive optical devices called phase retardation plates, or waveplates. Although traditionally fabricated from optically birefringent *solid* single crystal materials like quartz or mica, waveplates can be made from a class of *liquid* crystals called nematics. This article discusses the physical properties of nematic liquid crystals, their relationship to optical birefringence, and the potential advantages offered by nematic liquid crystal waveplates.

Of the various types of liquid crystals (cholesterics were discussed in Volume 5 of the LLE Review) nematic compounds have made the largest impact in the marketplace. Information displays using

Fig. 1a
Structure of nematic liquid crystal. A nematic liquid crystal molecule consists of carbon/hydrogen bonds connected by benzene rings. The properties of this compound, K15, are given in the text.

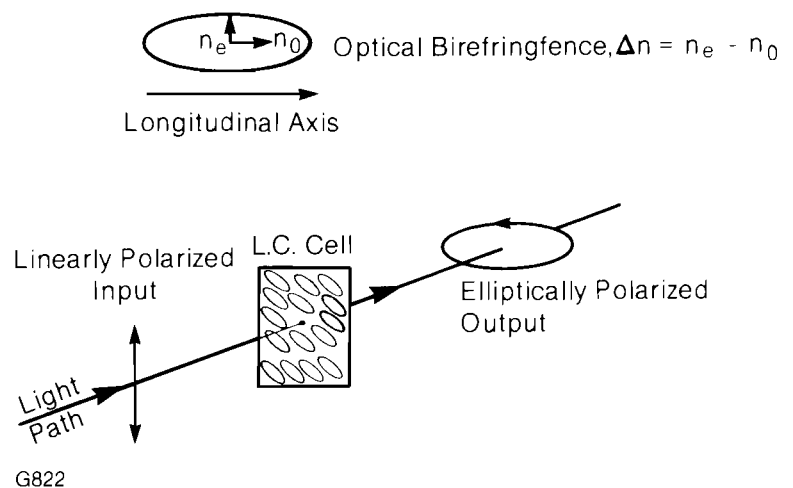
Fig. 1b
Alignment of liquid crystal molecules. In the nematic phase, all liquid crystal molecules align spontaneously through the bulk with their longitudinal axes parallel.



nematics are commonly found in digital watches, calculators, and electronic games.⁴ This commercial success is due to the unique physical properties of the nematic liquid crystal phase. Nematics possess the structure depicted in Fig. 1a, wherein chains of hydrocarbons are connected by benzene rings to form long, rigid, rodlike molecules. The most striking feature of nematics in bulk form is the tendency of these rodlike molecules to spontaneously align with their long axes parallel throughout their volume, as in Fig. 1b. The spatial order so obtained imparts crystalline behavior to the nematic, simultaneously preserving its fluid-like properties of low viscosity and flow. The composition and shape of nematic molecules and their preference for spontaneous alignment form the basis for their unique optical properties.

Fig. 2

Propagation of polarized light through nematic liquid crystal. Nematic liquid crystals exhibit a refractive index that depends upon the propagation direction and polarization vibration direction of incident light. Orthogonal components of linearly polarized light that enter a nematic vibrating in phase will emerge with one component's phase retarded with respect to the other. The emerging light will in general be elliptically polarized.



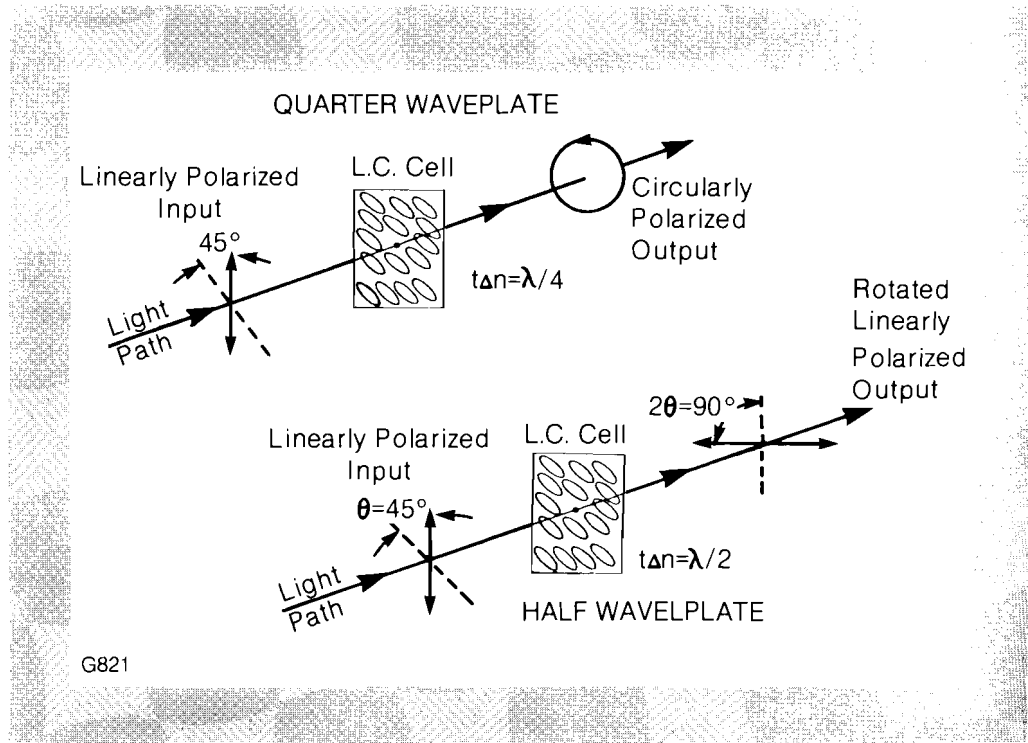
Nematic molecules are optically birefringent. Light incident upon a layer of oriented nematic fluid will propagate through it with a speed that depends upon whether the light polarization vibration direction is parallel or perpendicular to the long axes of the nematic molecules. As shown in Fig. 2, a nematic molecule resembles a uniaxial crystal in that it has two different refractive indices, n_o and n_e . Birefringence is defined as the difference between these two values, $\Delta n = n_e - n_o$. In nematics n_o may be larger or smaller than n_e . If it is larger, then light propagating through the liquid layer with a polarization vibration direction parallel to the long axes of the molecules travels more slowly than its orthogonal component. If the two components were in phase upon entering the liquid layer, they will be out of phase after leaving the liquid by an amount given by:

$$\delta = \frac{2\pi}{\lambda} t \Delta n$$

where δ is the amount of phase retardation, λ is the wavelength of optical radiation, and t is the thickness of birefringent material

traversed. This phase retardation is the key to the use of liquid crystals as waveplates.

Fig. 3
 Quarter waveplate and half waveplate conditions. In the special case where nematic liquid crystal thickness (t) times birefringence (Δn) equals a quarter wavelength, incident linearly polarized light will emerge circularly polarized. Incident linearly polarized light will emerge with its plane of polarization rotated by an angle 2θ when $t\Delta n$ equals one half wavelength.



G821

Two types of waveplates are required for the polarization manipulations described at the beginning of this article. Quarter waveplates convert linearly to circularly polarized light by introducing a 90 degree phase shift ($\delta=90^\circ$) to optical radiation, and half waveplates rotate the plane of vibration of linearly polarized light by introducing a 180 degree phase shift ($\delta=180^\circ$) (see Fig. 3). Table 1 gives the birefringence, and thickness required to fabricate half waveplates from nematics compared to quartz and mica at $\lambda = 1.05 \mu\text{m}$.

It is clear from Table 1 that nematics are order of magnitude more birefringent than solid crystalline materials. It is therefore necessary to produce liquid crystals in thin layers to achieve appropriate values of retardance.

Table 1
 Optical properties of nematics compared to quartz and mica for half waveplate applications at $\lambda = 1.05\mu$.

Material:	Mica	Quartz	Nematics
Δn :	0.003	0.0088	0.08 - 0.25
$t (\lambda/2), \mu\text{m}$:	175	60	6 - 2

G814

The components of nematic liquid crystal waveplates are shown in Fig. 4. Prior to assembling a cell as a liquid crystal sandwich with mylar spacers, the inner cell substrate surfaces must be rubbed unidirectionally with quarter micron diamond paste. This commonly prescribed technique⁵ forces the nematic molecules into alignment with their long axes parallel to the surfaces of the substrates. Thus anchored at each wall, the bulk of the nematic fluid spontaneously aligns as depicted in Fig. 4. With its rub direction oriented at 45° to the polarization direction of incident optical radiation, the cell functions as a waveplate, with capabilities not easily achieved with solid crystals.

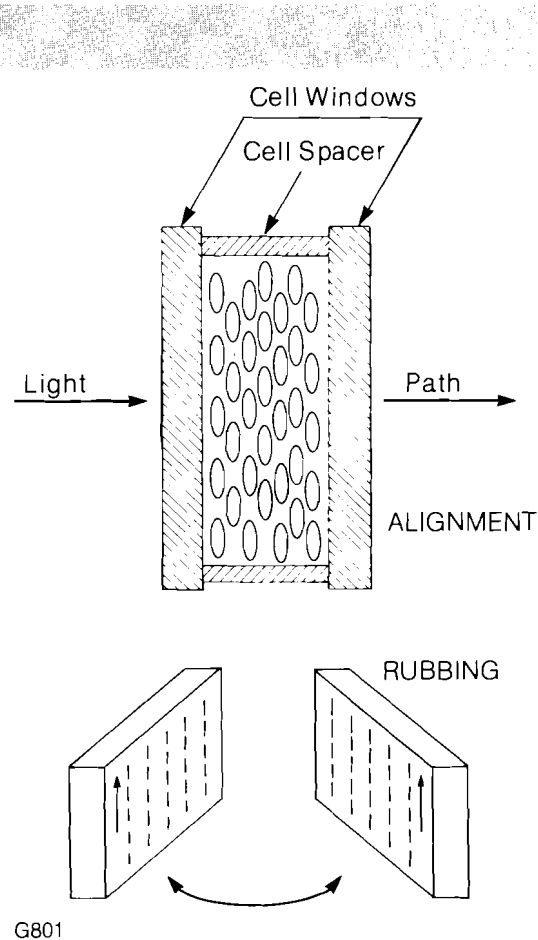
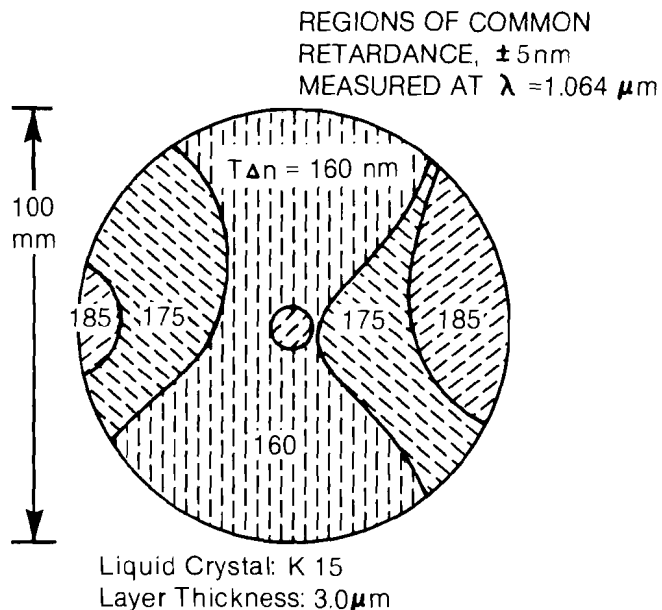


Fig. 4
Substrate support required for thin liquid crystal waveplates. A sandwich is made with the nematic fluid layer filling a gap between two glass plates whose separation is fixed with mylar spacers 1 - 10 μm thick. Molecular alignment parallel to the substrate surfaces is assured by unidirectionally rubbing the glass plates with diamond paste prior to assembly.

The primary advantage of nematic liquid crystals as waveplates is the ability to fabricate them in large sizes. Mica is very difficult to obtain in apertures larger than 1500 mm, and the availability of large stones of natural single crystal quartz with adequate optical quality has greatly diminished in the past 5 years. The useful aperture of a liquid crystal waveplate, however, is limited only by the dimensions of the glass substrates that comprise the cell. There is a problem in constructing cells whose liquid layer thickness is maintained at a constant value across the device

Fig. 5
Retardance contour plot of a 100 mm diameter liquid crystal waveplate. The problem of uniform retardance can be solved by the use of thicker windows. The BK-7 windows which comprise this cell were 9 mm thick.



G819

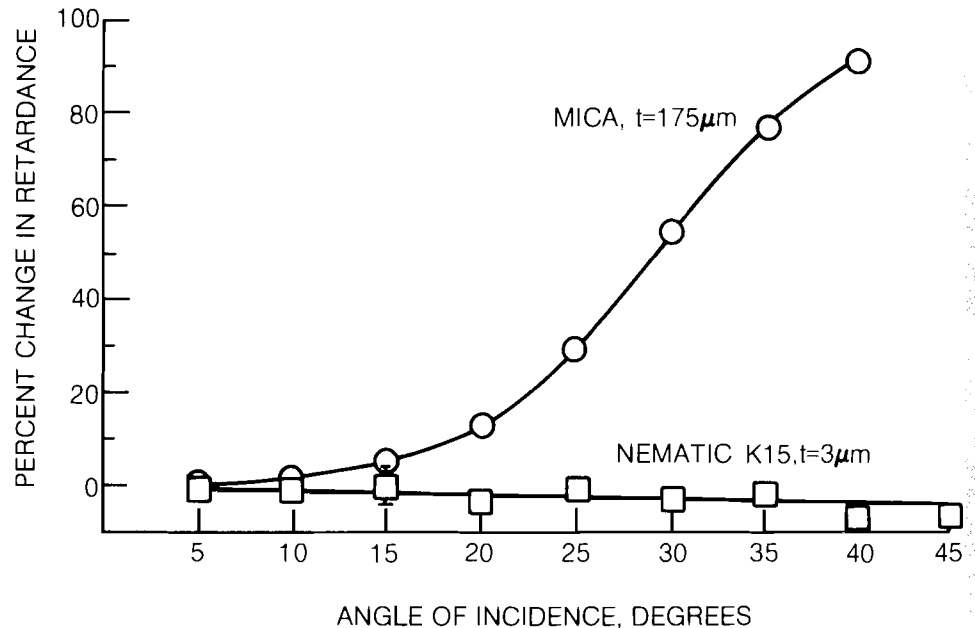
aperture. Figure 5 gives a contour plot measured on a 100 mm diameter liquid crystal cell whose glass substrates were not thick enough to support a uniform gap thickness of 6 μm. Cell windows with a lower aspect ratio and perhaps the use of nematics with a somewhat smaller birefringence (see Table 2) should enable larger devices with uniform retardance profiles to be constructed.

Vendor:	Merck	Hoffman LaRoche	BDH
Material:	ZLI-1646	TN-2080	K15
Viscosity, cst:	26	36	--
Temp. Range, °C:	-7 to +60	-5 to +72	24 to 35
Birefringence: n_e	1.565	1.610	1.702
@ $\lambda=0.589\mu\text{m}$ n_o	1.480	1.489	1.539
Δn	0.085	0.121	0.163

G815

Table 2
Properties of 3 commercial nematics used in the fabrication of waveplates at LLE. Note the birefringence ranges available and the temperature regions over which useful operations may be expected.

A second advantage to liquid crystals is the flexibility of design they offer in waveplate applications. Because of their large birefringence, thin liquid crystal layers provide the retardation required in most waveplate applications. This makes them less sensitive to the angle of incidence of incoming radiation than solids (see Fig. 6). A large acceptance angle relaxes alignment requirements in laser system applications.



G818

Fig. 6
Retardance versus angle of incidence. Liquid crystal waveplates exhibit minimal angular sensitivity when compared to solid crystal alternatives. Measurements made with a 1 mm diameter CW:Yag laser show the nematic K15 to be insensitive to angle of incidence when compared to mica.

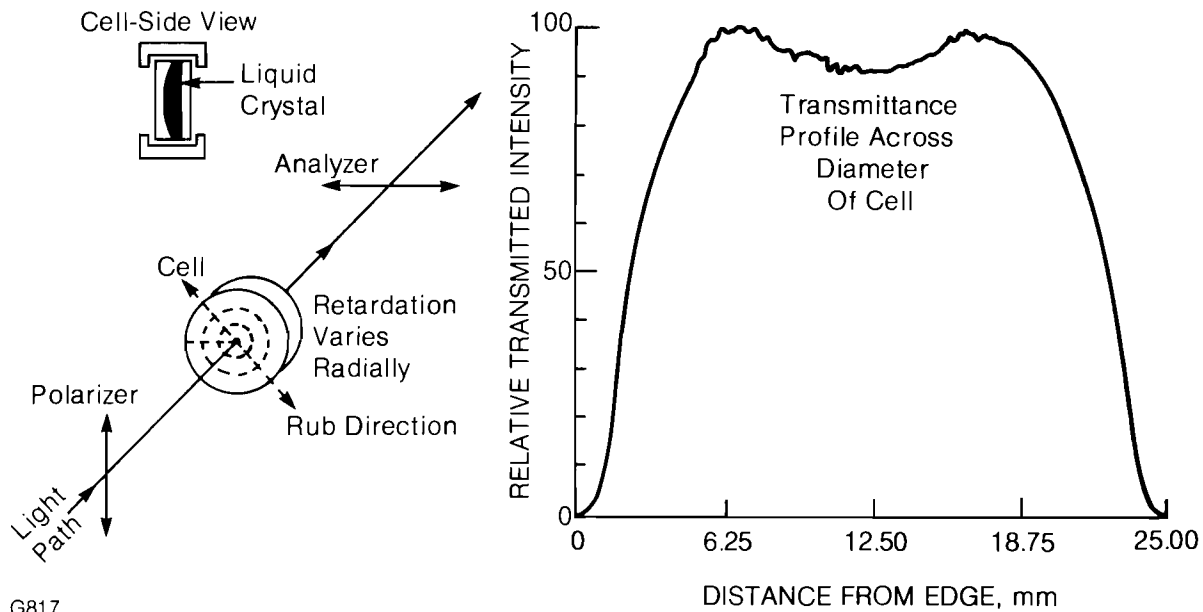
This design flexibility is also evident in the application of liquid crystals as radially birefringent waveplates. Figure 7 shows how, by putting a few waves of curvature on the inner surface of a glass flat, one can then assemble a cell whose liquid thickness (and therefore cell retardance) decreases radially from center to edge. Weak birefringent lenses composed of crystal quartz have recently been proposed as a means for constructing soft apertures for lasers.⁶ By index matching to the substrate, a liquid crystal radially birefringent element would remove the requirement for a correcting lens in such a scheme.

This article has explained how the nematic class of liquid crystal compounds might be used to fabricate waveplates for large aperture laser systems. Some of the advantages to the use of liquid crystals in place of solid crystals have been discussed. Preliminary measurements have shown that, although more work is required, liquid crystals can be aligned over large areas and oriented to operate as waveplates. The laser damage threshold of liquid crystals and their potential for use at other wavelengths will be the subject of future research.

REFERENCES

1. W. Seka, J. Soures, O. Lewis, J. Bunkenburg, D. Brown, S. Jacobs, G. Mourou, and J. Zimmerman, *Appl. Opt.* **19** 409-419 (1980).
2. L. L. Steinmetz, T. W. Pouliot, and B. C. Johnson, *Appl. Opt.* **12** 1468-1471 (1973).

3. G. Mourou, J. Bunkenburg, and W. Seka *Optics Communications* **34** 252-254 (1980).
4. See, for example *The Physics and Chemistry of Liquid Crystal Devices*, Ed. by Gerald J. Sprockel, Plenum Press, New York, 1980.
5. G. Meir, E. Sackman, and J. G. Grabmaier, *Applications of Liquid Crystals* **99**, Springer Verlag, New York, 1975.
6. G. Giuliani, Y. K. Park, and R. L. Byer, *Optics Letters* **5** 491-493 (1980).



G817

Fig. 7
Fabrication of waveplates with radially varying retardance. Liquid crystals may be used to construct waveplates with radially varying retardance. Filling the air gap between a weak lens and a flat, a liquid crystal radially birefringent element could serve in conjunction with a polarizer as a soft aperture. The transmittance profile for a 25 mm diameter cell oriented between crossed polarizers and scanned across its diameter using a 1 mm CW:Yag laser beam, shows that an internal sag of $8 \mu\text{m}$ is adequate to give just over one half wave of retardation at cell center using nematic TN-2080.

1.C Active-Passive Mode-Locked Oscillator Generating Nanosecond Pulses

Laser oscillators operating at $1.054 \mu\text{m}$ are needed to drive phosphate-based glass laser amplifier chains optimally. For explosive pusher mode laser fusion experiments, one of the important parameters is peak power. Consequently, short pulse oscillators have been designed which operate reliably between 50 psec and 600 psec FWHM pulse duration.¹ Recent advances towards ablative or quasi-ablative target compressions² and high efficiency frequency conversions³ have made reliable optical oscillators generating pulses between 1 nsec and 1.2 nsec duration necessary. Actively mode-locked oscillators fulfill this requirement; they offer high repetition rates, quick tuning of the pulse duration, and very good pulse duration and amplitude stability.⁴ Their disadvantage, however, is high cost largely due to

a complicated electronic package compared to an LC-discharge network driving a conventional oscillator. Operating a passive oscillator in the monomode regime⁵ is also possible, but the reproducibility and absence of substructures in the pulse are often not considered sufficient for target irradiation experiments. Regenerative amplifier^{6,7} systems are able to produce injection-locked pulses which can be stretched up to 1.5 nsec FWHM; at that duration, however, their amplitude stability is not yet truly satisfactory.

The Laboratory for Laser Energetics has developed an active-passive mode-locked oscillator with much the same characteristics of earlier oscillators,¹ which is capable of generating optical pulses of up to 1.4 nsec duration.

Presently, the oscillator described in Ref. 1 is used in the University of Rochester's laser systems GDL⁸ and OMEGA.⁹ Though very reliable as a short pulse oscillator, pulses longer than 700 psec cannot be achieved with the required stability and absence of substructures. The reason for this limit can be understood as follows:

- For a cavity length of 1.5 m and a gain bandwidth of 20 nm, the laser runs on about 2.5×10^4 longitudinal modes when pumped 20% above threshold.
- An etalon with a finesse of 2 and an optical thickness of 5.88 mm restricts the FWHM bandwidth to approximately 0.048 nm so that the laser will run on about 65 modes. With such a laser we observe still reproducible pulses of <700 psec duration. If the number of modes drops much below the above value however, one finds incomplete mode-locking, poor stability, satellite pulses, and occasional no lases.

In order to further restrict the lasing bandwidth without restricting the number of modes on which the laser is running, the cavity length has to be increased. Therefore, doubling the cavity length limits the bandpass by a factor of two (e.g., an etalon with finesse = 2, thickness = 8, index = 1.47) while maintaining the number of modes and hence the major stability characteristics of the oscillator.

Apart from the thickest etalon as a bandwidth-restricting element, the laser contains two bandwidth-generating elements, namely the dye and the AO (acousto-optic) modulator. The pulse duration τ_{AO} , resulting from etalon and AO modulator only, can be calculated quite well using the theory for active mode-locking described in Ref. 10. Differences between theory and experiment arise from a lack of buildup time to ensure Fourier transform-limited mode-locking.^{11,12} The pulse duration τ_D resulting from etalon and dye only is much harder to calculate as the process of the transient mode-locking of a gradually bleaching dye is very complex and we are not aware of a closed form solution to this problem. The contribution of dye and etalon to the pulse duration, however,

can easily be measured. The final pulse duration due to both processes can, assuming Gaussian pulses in each case be obtained via:

$$\frac{1}{\tau^2} = \frac{1}{\tau_{AO}^2} + \frac{1}{\tau_D^2}$$

Our 1.5 m oscillator as well as our 3 m oscillator when Q-switched with a slow dye follow this relationship closely.

The experimental layout is shown in Fig. 8. To keep the laser cavity within manageable dimensions, we used two dielectric mirrors (R_{max} at 45°) to fold the cavity.

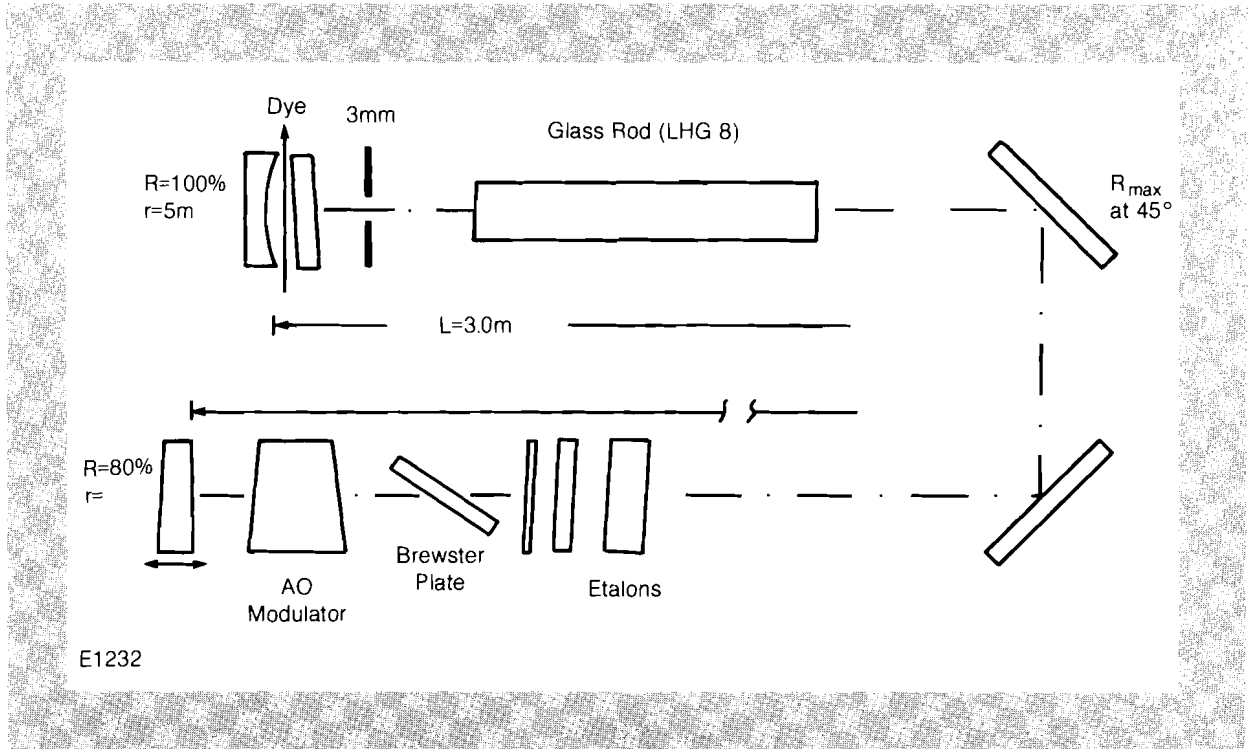


Fig. 8
Schematic layout of the oscillator cavity. An oscillator capable of generating optical pulses up to 1.4 nsec was built with only small modification of a 600 psec oscillator.

The pump cavity was a double elliptical unit (Raytheon LC-73) which uses two FX6-81-C4 flashlamps in series. A pulse forming network was used to form a current pulse of about 240 μ sec duration discharged through the flashlamps. This current pulse makes it possible to increase the fluorescence power from the laser rod more gradually, such that the nonlinear bleaching phase of the dye becomes as long as possible. This ensures a maximum number of passes through the AO modulator, hence the closest approach to complete mode-locking during the lasing-buildup phase.^{11,12}

The laser was Q-switched with a slow Ni dye (Eastman Kodak Ni dye #14015) such that the contribution of the dye to the shortening of individual pulses was less than that of the modulator. Accordingly, the modulator dominates the observed pulse duration.

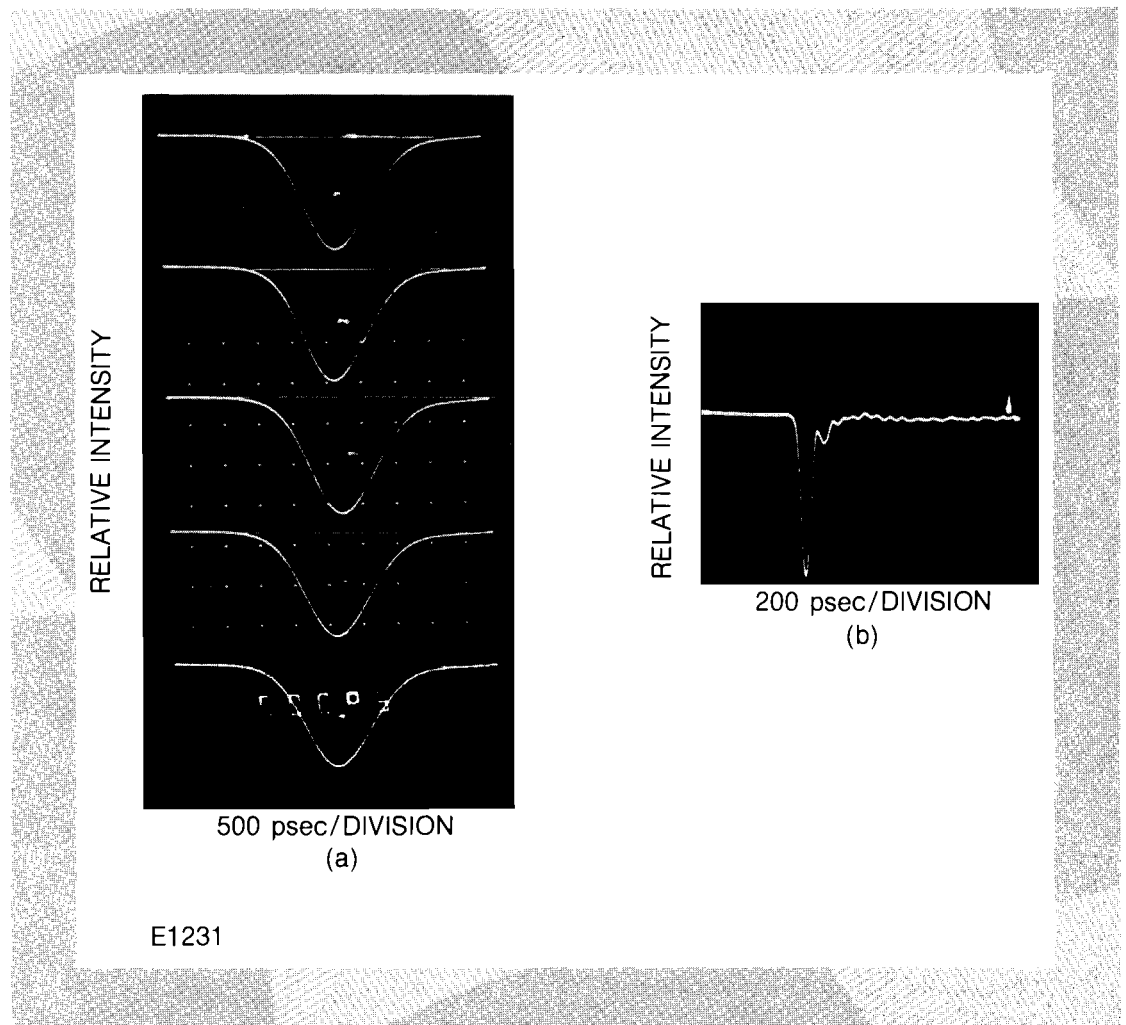


Fig. 9a

Laser output pulses. Shown are five consecutive shots. The oscillator exhibits amplitude stability of $\pm 4\%$.

Fig. 9b

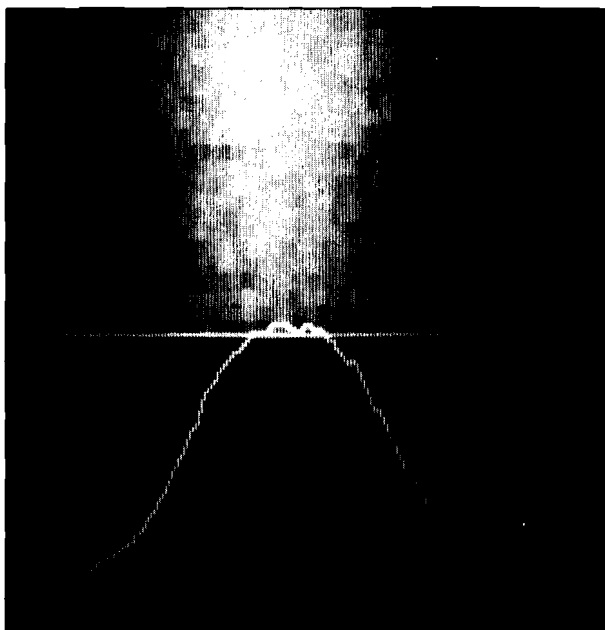
Response time of the detector and scope.

Figure 9a shows a sequence of five consecutive shots, the response of the detection system is shown in Fig. 9b. The pulse duration is 1.15 ± 0.06 nsec, the relative amplitude stability of the envelope of the output train was measured to be $\pm 4\%$, with single pulse energies up to 0.6 mJ. Figure 10 shows a streak of the frequency-doubled pulse which verifies the absence of sub-structures in the red pulse to within 2% amplitude modulation.

Only relatively small modifications to a 1.5 m cavity¹ are needed to achieve these results. From the theoretical considerations, it can be expected that the limit of the system is a pulse of 1.4 nsec duration, obtainable with BK7 etalons of finesse 2 and 8 mm thickness. The separation between pulses of 20 nsec provides for easy single pulse switch out. This oscillator represents a useful addition to the possibilities of generating a stable mode-locked laser pulse in the nanosecond regime.

REFERENCES

1. W. Seka, J. Bunkenburg, *J. Appl. Phys.* **49**, 2277 (1978).



E1230

Fig. 10

Streak record of the frequency doubled single 1.15 nsec pulse. Streaks of the frequency doubled pulse verify the absence of substructures in the red pulse to within 2% amplitude modulation.

2. C. E. Max, C. E. McKee, and W. C. Mead, *Phys. Rev. Lett.* **45**, 28 (1980).
3. W. Seka, S. D. Jacobs, J. E. Rizzo, R. Boni, and R. S. Craxton; accepted for publication by *Opt. Comm.*
4. D. J. Kuizenga, *Opt. Comm.* **22**, 156 (1977).
5. A. E. Egorov, V. V. Korobkin, R. V. Serov, *Sov. J. Quant. Electron.*, **5**, 3 (1975).
6. W. H. Lowdermilk, J. E. Murray, D. C. Downs; *LLNL Report UCRL-50021-74* pp. 2-300-308.
7. G. Albrecht and G. Mourou, submitted to *IEEE J.Q.E.* special issue on lasers for fusion.
8. W. Seka, J. Soures, O. Lewis, J. Bunkenburg, D. Brown, S. Jacobs, G. Mourou, and J. Zimmerman, *Appl. Opt.* **19**, (1980).
9. J. Bunkenburg, W. Seka, J. Soures, submitted to *IEEE J.Q.E.* special issue on lasers for fusion.
10. D. J. Kuizenga, A. E. Siegman, *IEEE J.Q.E.* **6**, 694 (1970).
11. D. J. Kuizenga, D. W. Phillion, T. D. Lund, A. E. Siegman, *Opt. Comm.* **9**, 221 (1973).
12. A. E. Siegman, D. J. Kuizenga, *Opto Electric* **6**, 43 (1974).

1.D GDL Facility Report

The GDL facility continued a high level of operation during the second quarter of FY 81.

A total of 759 shots were delivered by this facility in the period 1 January – 31 March, 1981. The shot distribution was as follows:

3 ω Target Experiments	174 Shots
3 ω Diagnostics c/o	59
3 ω Beam Characterization	42
Damage Test Facility	453
X-Ray Program	31
Total	759 Shots

Details of some of this quarter's work are presented elsewhere in this volume. One of the primary elements of the experimental program on GDL during this time was the 0.35 μm interaction program. Measurements were made of the target absorption with both long (450 psec) and short (100 psec) pulses, the time and spectrally resolved stimulated Brillouin backscatter, x-ray line conversion efficiency, stimulated Raman backscatter, burn through depth (using x-ray spectroscopy), time resolved x-ray emission, x-ray continuum plasma blow-off ion velocity distribution, and beam intensity distribution on target.